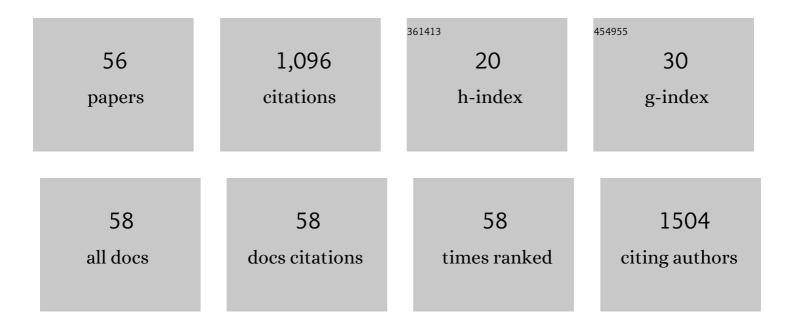
Yoichi Takakusagi

List of Publications by Year in descending order

Source: https://exaly.com/author-pdf/5643362/publications.pdf Version: 2024-02-01



#	Article	IF	CITATIONS
1	The natural sulfoglycolipid derivative SQAP improves the therapeutic efficacy of tissue factor-targeted radioimmunotherapy in the stroma-rich pancreatic cancer model BxPC-3. Translational Oncology, 2022, 15, 101285.	3.7	1
2	Structure-guided design enables development of a hyperpolarized molecular probe for the detection of aminopeptidase N activity in vivo. Science Advances, 2022, 8, eabj2667.	10.3	10
3	Design of Nuclear Magnetic Resonance Molecular Probes for Hyperpolarized Bioimaging. Angewandte Chemie - International Edition, 2021, 60, 14779-14799.	13.8	22
4	Entwicklung molekularer Sonden für die hyperpolarisierte NMRâ€Bildgebung im biologischen Bereich. Angewandte Chemie, 2021, 133, 14904-14925.	2.0	0
5	Phage display technology for target determination of small-molecule therapeutics: an update. Expert Opinion on Drug Discovery, 2020, 15, 1199-1211.	5.0	11
6	Biosensor-based High Throughput Biopanning and Bioinformatics Analysis Strategy for the Global Validation of Drug-protein Interactions. Journal of Visualized Experiments, 2020, , .	0.3	1
7	Design strategy for serine hydroxymethyltransferase probes based on retro-aldol-type reaction. Nature Communications, 2019, 10, 876.	12.8	31
8	Intratumoral evaluation of 3D microvasculature and nanoparticle distribution using a gadolinium-dendron modified nano-liposomal contrast agent with magnetic resonance micro-imaging. Nanomedicine: Nanotechnology, Biology, and Medicine, 2018, 14, 1315-1324.	3.3	9
9	Rational Design of [¹³ C,D ₁₄] <i>Tert</i> â€butylbenzene as a Scaffold Structure for Designing Longâ€lived Hyperpolarized ¹³ C Probes. Chemistry - an Asian Journal, 2018, 13, 280-283.	3.3	8
10	Hyperpolarized [1-13C]-Pyruvate Magnetic Resonance Spectroscopic Imaging of Prostate Cancer <i>In Vivo</i> Predicts Efficacy of Targeting the Warburg Effect. Clinical Cancer Research, 2018, 24, 3137-3148.	7.0	36
11	Radiotherapy Synergizes with the Hypoxia-Activated Prodrug Evofosfamide: In Vitro and In Vivo Studies. Antioxidants and Redox Signaling, 2018, 28, 131-140.	5.4	27
12	A Multimodal Molecular Imaging Study Evaluates Pharmacological Alteration of the Tumor Microenvironment to Improve Radiation Response. Cancer Research, 2018, 78, 6828-6837.	0.9	16
13	Metabolic and Physiologic Imaging Biomarkers of the Tumor Microenvironment Predict Treatment Outcome with Radiation or a Hypoxia-Activated Prodrug in Mice. Cancer Research, 2018, 78, 3783-3792.	0.9	42
14	Using the QCM Biosensor-Based T7 Phage Display Combined with Bioinformatics Analysis for Target Identification of Bioactive Small Molecule. Methods in Molecular Biology, 2018, 1795, 159-172.	0.9	2
15	Design of a 15N Molecular Unit to Achieve Long Retention of Hyperpolarized Spin State. Scientific Reports, 2017, 7, 40104.	3.3	39
16	A Strategy to Design Hyperpolarized ¹³ C Magnetic Resonance Probes Using [1â€ ¹³ C]αâ€Amino Acid as a Scaffold Structure. Chemistry - an Asian Journal, 2017, 12, 949-953.	3.3	12
17	Direct Monitoring of γâ€Glutamyl Transpeptidase Activity In Vivo Using a Hyperpolarized 13 Câ€Labeled Molecular Probe. Angewandte Chemie, 2016, 128, 10784-10787.	2.0	7
18	Direct Monitoring of γâ€Clutamyl Transpeptidase Activity In Vivo Using a Hyperpolarized ¹³ Câ€Labeled Molecular Probe. Angewandte Chemie - International Edition, 2016, 55, 10626-10629.	13.8	40

Үоісні Такакизаді

#	Article	IF	CITATIONS
19	Effect of ionic interaction between a hyperpolarized magnetic resonance chemical probe and a gadolinium contrast agent for the hyperpolarized lifetime after dissolution. Journal of Magnetic Resonance, 2016, 270, 157-160.	2.1	1
20	Design of a Hyperpolarized Molecular Probe for Detection of Aminopeptidase N Activity. Angewandte Chemie, 2016, 128, 1797-1800.	2.0	10
21	Design of a Hyperpolarized Molecular Probe for Detection of Aminopeptidase N Activity. Angewandte Chemie - International Edition, 2016, 55, 1765-1768.	13.8	36
22	Design of a hyperpolarized ¹⁵ N NMR probe that induces a large chemical-shift change upon binding of calcium ions. Chemical Communications, 2015, 51, 12290-12292.	4.1	25
23	Pyruvate sensitizes pancreatic tumors to hypoxia-activated prodrug TH-302. Cancer & Metabolism, 2015, 3, 2.	5.0	69
24	13C-MR Spectroscopic Imaging with Hyperpolarized [1-13C]pyruvate Detects Early Response to Radiotherapy in SCC Tumors and HT-29 Tumors. Clinical Cancer Research, 2015, 21, 5073-5081.	7.0	54
25	Ridaifen C, tamoxifen analog, is a potent anticancer drug working through a combinatorial association with multiple cellular factors. Bioorganic and Medicinal Chemistry, 2015, 23, 6118-6124.	3.0	6
26	Multimodal biopanning of T7 phage-displayed peptides reveals angiomotin as a potential receptor of the anti-angiogenic macrolide Roxithromycin. European Journal of Medicinal Chemistry, 2015, 90, 809-821.	5.5	9
27	Pyruvate Induces Transient Tumor Hypoxia by Enhancing Mitochondrial Oxygen Consumption and Potentiates the Anti-Tumor Effect of a Hypoxia-Activated Prodrug TH-302. PLoS ONE, 2014, 9, e107995.	2.5	35
28	<i>In Vivo</i> Imaging of Tumor Physiological, Metabolic, and Redox Changes in Response to the Anti-Angiogenic Agent Sunitinib: Longitudinal Assessment to Identify Transient Vascular Renormalization. Antioxidants and Redox Signaling, 2014, 21, 1145-1155.	5.4	41
29	Ridaifen B, a tamoxifen derivative, directly binds to Grb10 interacting GYF protein 2. Bioorganic and Medicinal Chemistry, 2013, 21, 311-320.	3.0	14
30	Mapping a Disordered Portion of the Brz2001-Binding Site on a Plant Monooxygenase, DWARF4, Using a Quartz-Crystal Microbalance Biosensor-Based T7 Phage Display. Assay and Drug Development Technologies, 2013, 11, 206-215.	1.2	7
31	Identification and Characterization of the Direct Interaction between Methotrexate (MTX) and High-Mobility Group Box 1 (HMGB1) Protein. PLoS ONE, 2013, 8, e63073.	2.5	35
32	Exploration of the binding proteins of perfluorooctane sulfonate by a T7 phage display screen. Bioorganic and Medicinal Chemistry, 2012, 20, 3985-3990.	3.0	7
33	The antitumor agent doxorubicin binds to Fanconi anemia group F protein. Bioorganic and Medicinal Chemistry, 2012, 20, 6248-6255.	3.0	15
34	Binding region and interaction properties of sulfoquinovosylacylglycerol (SQAG) with human vascular endothelial growth factor 165 revealed by biosensor-based assays. MedChemComm, 2011, 2, 1188.	3.4	7
35	Characterization of marine X-family DNA polymerases and comparative analysis of base excision repair proteins. Biochemical and Biophysical Research Communications, 2011, 415, 193-199.	2.1	6
36	A Screening of a Library of T7 Phage-Displayed Peptide Identifies E2F-4 as an Etoposide-Binding Protein. Molecules, 2011, 16, 4278-4294.	3.8	11

Үоісні Такакизаді

#	Article	IF	CITATIONS
37	Heterogeneous Nucleation of Protein Crystals on Fluorinated Layered Silicate. PLoS ONE, 2011, 6, e22582.	2.5	21
38	Camptothecin (CPT) directly binds to human heterogeneous nuclear ribonucleoprotein A1 (hnRNP A1) and inhibits the hnRNP A1/topoisomerase I interaction. Bioorganic and Medicinal Chemistry, 2011, 19, 7690-7697.	3.0	21
39	Screening of a library of T7 phage-displayed peptides identifies alphaC helix in 14-3-3 protein as a CBP501-binding site. Bioorganic and Medicinal Chemistry, 2011, 19, 7049-7056.	3.0	12
40	Foam fractionation of protein: Correlation of protein adsorption onto bubbles with a pH-induced conformational transition. Analytical Biochemistry, 2011, 419, 173-179.	2.4	28
41	A sulfoglycolipid beta-sulfoquinovosyldiacylglycerol (ÂSQDG) binds to Met1-Arg95 region of murine DNA polymerase lambda (Mmpol Â) and inhibits its nuclear transit. Protein Engineering, Design and Selection, 2010, 23, 51-60.	2.1	8
42	Use of phage display technology for the determination of the targets for small-molecule therapeutics. Expert Opinion on Drug Discovery, 2010, 5, 361-389.	5.0	35
43	Identification of trimannoside-recognizing peptide sequences from a T7 phage display screen using a QCM device. Bioorganic and Medicinal Chemistry, 2009, 17, 195-202.	3.0	20
44	DNA polymerase mu interacts with a meiosis-specific RecA homolog Lim15 during meiosis in Coprinus cinereus. Biochemical and Biophysical Research Communications, 2009, 390, 32-37.	2.1	0
45	Identification of a methotrexate-binding peptide from a T7 phage display screen using a QCM device. Bioorganic and Medicinal Chemistry, 2008, 16, 7410-7414.	3.0	14
46	Efficient one-cycle affinity selection of binding proteins or peptides specific for a small-molecule using a T7 phage display pool. Bioorganic and Medicinal Chemistry, 2008, 16, 9837-9846.	3.0	24
47	Use of layer silicate for protein crystallization: Effects of Micromica and chlorite powders in hanging drops. Analytical Biochemistry, 2008, 373, 322-329.	2.4	17
48	Identification of Small Molecule Binding Molecules by Affinity Purification Using a Specific Ligand Immobilized on PEGA Resin. Bioconjugate Chemistry, 2008, 19, 2417-2426.	3.6	17
49	Coenzyme Q10 as a potent compound that inhibits Cdt1–geminin interaction. Biochimica Et Biophysica Acta - General Subjects, 2008, 1780, 203-213.	2.4	8
50	Chemical properties of fatty acid derivatives as inhibitors of DNA polymerases. Organic and Biomolecular Chemistry, 2007, 5, 3912.	2.8	11
51	Identification of C10 biotinylated camptothecin (CPT-10-B) binding peptides using T7 phage display screen on a QCM device. Bioorganic and Medicinal Chemistry, 2007, 15, 7590-7598.	3.0	24
52	Lariatins, Novel Anti-mycobacterial Peptides with a Lasso Structure, Produced by Rhodococcus jostii K01-B0171. Journal of Antibiotics, 2007, 60, 357-363.	2.0	80
53	Two X family DNA polymerases, λ and μ, in meiotic tissues of the basidiomycete, Coprinus cinereus. Chromosoma, 2007, 116, 545-556.	2.2	11
54	Total Synthesis of (-)-Neoechinulin A. Synlett, 2006, 2006, 0677-0680.	1.8	1

#	Article	IF	CITATIONS
55	Camptothecin binds to a synthetic peptide identified by a T7 phage display screen. Bioorganic and Medicinal Chemistry Letters, 2005, 15, 4850-4853.	2.2	24
56	Synthesis of a biotinylated camptothecin derivative and determination of the binding sequence by T7 phage display technology. Bioorganic and Medicinal Chemistry Letters, 2005, 15, 4846-4849.	2.2	17